The LS-TaSC™ Tool
THEORY MANUAL

08/21/15 (r:6719)
LS-TaSC Dev

LIVERMORE SOFTWARE TECHNOLOGY CORPORATION (LSTC)

Corporate Address
Livermore Software Technology Corporation
P. O. Box 712
Livermore, California 94551-0712

Support Addresses
Livermore Software Technology Corporation
7374 Las Positas Road
Livermore, California 94551
Tel: 925-449-2500 ♦ Fax: 925-449-2507
Email: sales@lstc.com
Website: www.lstc.com

Livermore Software Technology Corporation
1740 West Big Beaver Road
Suite 100
Troy, Michigan 48084
Tel: 248-649-4728 ♦ Fax: 248-649-6328

Disclaimer

Issue Date: 21/01/2002

This file contains the code for implementing the key schedule for AES (Rijndael) for block and key sizes of 16, 24, and 32 bytes.

TABLE OF CONTENTS

TABLE OF CONTENTS 0-3

1 Introduction 1-2

1.1 Topology design methods 1-2

1.2 Topology design for crashworthiness – a review 1-3

2 Material parameterization and interpolation schemes 1-5

2.1 Preliminaries 1-5

2.1.1 Isotropic elasticity 1-5

2.1.2 Fundamentals of mixtures 1-6

2.2 Solid isotropic material with penalization 1-7

2.2.1 Extension to elasto-plasticisty 1-7

2.3 Hashin-Shtrikman bounds 1-8

2.4 Material parameterization of shell structures 1-9

3 Filtering 1-10

3.1 Linear filter 1-11

3.2 Weighting functions 1-11

4 Problem formulation 1-12

4.1 The global optimization problem 1-12

4.2 The local design problem 1-13

5 Design algorithm 1-14

5.1 Design initialization 1-16

5.2 Response analysis 1-16

5.3 Global variable update using control theory 1-17

5.4 Global variable update via mathematical programming 1-18

5.5 Local variable update 1-18

5.5.1 Internal energy density – two interpretations 1-19

5.6 Stopping criteria 1-19

6 References 1-21

“I must say it looks a bit like science fiction to many people”
Ofir Shor while evaluating the α-version in June 2009

1 Introduction

Topology optimization, also referred to as layout or generalized shape optimization, is aimed at finding the best arrangement of material in a fixed domain in a way that predefined performance merits are satisfied. In the structural design synthesis, topology optimization is primarily used in the conceptual design phase and the boundary of the obtained topology is often adjusted using shape optimization. The field of structural topology optimization has been extensively studied since the late 1980s, see e.g., the monographs of Rozvany [1], Rozvany and Olhoff [2], Bendsøe and Sigmund [3], the contemporary and comprehensive surveys of Eschenauer and Olhoff [4], van Dijk *et al.* [5], and the references therein. The goal of this chapter is limited to provide the reader with a compendium of the key ideas LS-TaSC is built upon.

1.1 Topology design methods

Topology design methods are best classified as discrete and continuous approaches. The *discrete formulation of topology design* relies on the assumption that the optimal topology of the structure is described by the macroscopic variation of material (1) and void (0) phases. The optimum topology or layout design problem, in its essence, consist of determining the optimal number, position, and mutual connectivity of the structural members [4]. It is shown that the resulting 0/1 integer programming problem is not well-posed in the continuum settings which entails the need of some sort of regularization of the original problem [6], see e.g. [7]. Existence studies, however, indicate that non-convergent, minimizing sequences of admissible designs with finer and finer geometrical details, see [8], [9], [10] and also the results in [11], can be found for the original 0/1 problem which, in the limit, should be interpreted as composites made from the original constituents and as such are integral parts of the optimal structure [3]. The previous finding breathed new life into the field and led to popular continuous topology design approaches.
In *continuous or continuum topology formulations*, the material at a spatial point $\boldsymbol{x} \in \Omega_D$, where Ω_D is a fixed design domain, need not be strictly one of the composing materials but may instead be some mixture of them. Various forms of material mixtures, also called composites, are routinely permitted to exist throughout the design domain in intermediate as well as final design states [12]. Continuum topology formulation methods allow us to

convert a topology design problem with 0/1 integer, also called black and white or solid-void, material parameterization to a sizing problem by virtue of material interpolation schemes. The number of variables in the resulting sizing problem is proportional to the number of elements or nodes in the discretization of the fixed design domain. Therefore topology design problems typically require the efficient solution of an optimization problem with orders of magnitude more design variables than constraints.
Continuum topology formulations can be classified as relaxation and restriction based methods. In *relaxation methods*, an assumed micro-structure is invoked ab initio, i.e. the design space is extended to include parameters uniquely defining the micro-structure, and effective material properties are computed using a homogenization technique. Frequently utilized micro-morphologies include periodic porous media [13], rank-2 laminates [14], dilute suspensions of ellipsoidal particles [15], and two-phase composites [16]. In *restriction methods*, no assumptions on the underlying micro-structures are made but the space of admissible designs is restricted in the problem formulation that renders the topology optimization problem well-posed. Proposed restriction techniques may be classified as constraint methods [17], [18], [19], [20], [21], [22], filtering techniques [23], [24], [25], [26], level-set methods [27], [5], and alternative approaches, see e.g., [28], [29]. An excellent comparative study on restriction methods in topology optimization is given by Borrvall [22]. Although material distributions with local mixtures are omitted in most applications, a micro-structure with prescribed effective properties may be obtained using an inverse homogenization method also called as *material design* [30], [16].

1.2 Topology design for crashworthiness – a review

Crashworthiness design is an emerging discipline that combines vehicle crash simulations and novel design optimization techniques and thereby entails one of the most difficult engineering endeavor to date [31]. The motivation is to improve occupant and pedestrian safety subject to material, manufacturing, and other cost functions. Perhaps the greatest challenge of crashworthiness design is to accurately model the complex (multi-)physical phenomenon involved in a crash event. These, among others, include geometric and material nonlinearities, general contact, time-dependent boundary conditions, and progressive damage behavior. Other important aspects of vehicle crash simulations are the efficacy and scalability of distributed solvers and (real-time) visualization tools.
In the design synthesis, the aim is ideally to find a robust solution to a multi-objective or multi-modal, nonlinear, and nonconvex optimization problem with potentially millions of design variables and several local as well as global constraints. In view of the available computational hardware and the shortness of a design cycle, the latter objective is currently intractable. Present approaches instead either utilize a few design parameters and determine a robust design by virtue of response surface methodologies, see e.g., [32], or use direct optimization methods in combination with other heuristic search techniques to find a feasible solution to a problem described by a large set of design variables. One also needs to be careful when formulation the design problem which often involves conflicting objectives. For example, keeping the accelerations exerted to the occupant below injury levels and limiting the intrusion into the passenger compartment to a inhibit chest, head, and limb injuries is just one the design controversies [33]. Topology design for

crashworthiness is still in its infancy with very limited published research. In what follows, a brief summary of the previous works is given.

In their seminal work on structural crashworthiness design, Mayer *et al.* [34] proposed to maximize the energy absorption of shell structures in a nonlinear finite element analysis (FEA) invoking a relaxation formulation of topology optimization. A simple porous periodic micro-morphology is assumed and effective elastic as well as plastic hardening moduli at intermediate densities are obtained via homogenization. Crashworthiness topology design of frame structures is investigated by Pedersen [35], [36]. The objective of the latter works is to minimize the relative error between the current and desired structural responses sampled at predefined time steps. The ground structure is modelled using beam elements with plastic hinges and the simulation was carried out in a quasi-static sense neglecting contact between the different members. The listed simplifications, while certainly limit the applicability of the method, permit the use of design sensitivities calculus and continuous mathematical programming.

Inspired by the works of Mayer *et al.* [34] and Ebisugi *et al.* [37], Soto [33] devised a heuristic design approach based on the concepts of prescribed plastic strain/stress criterion and controlled crash behavior. While the former idea provides the designer with a mean to control energy absorption within the structure, the latter includes constraints on the acceleration as equalities in the state equations and thereby automatically ensures their exact satisfaction during the design cycle. An alternative heuristic continuum topology optimization technique integrating cellular automaton based local design update rules with FEA is proposed to solve crashworthiness problems by Patel [38] and Patel *et al.* [31]. The crux of the method is to achieve uniform prescribed internal energy density, and as a consequence energy absorption, within the entire structure. Concurrently, Forsberg and Nilsson [39] proposed to formulate the uniform internal energy density criterion as a min-max problem. The use of the internal energy density in structural optimization, its relationship with the design sensitivity information for crash problems, and its usefulness for ranking variables is extensively studied by Öman and Nilsson [40], [41].

More recently, an topology design scheme using equivalent static loads is introduced by Motamarri *et al.* [42] and Ramani and Kaushik [43]. Conceptually, the nonlinear dynamic problem is replaced and solved as a linear optimization problem with multiple static load cases in each design iteration. Although the approach is found to be efficient in problems with moderate nonlinearities, it falls short in general crashworthiness design problems [44].

The remaining part of this manuscript is organized as follows. Material parameterization and interpolation schemes are discussed in section 2. A brief overview on filtering methods is provided in section 3. Finally, the topology design formulation and the solution scheme proposed in LS-TaSC is presented in sections 4 and 5, respectively.

2

Material parameterization and interpolation schemes

Material interpolation schemes derived from well-known mixing rules play a dominant role in the current release of LS-TaSC and are reviewed in this section. For more details on the subject, the reader is advised to consult Bendsøe and Sigmund [3], [45], and references therein. To set the scene for the discussion on material interpolation schemes, some key concepts are revisited in section 2.1. Material interpolation schemes utilized in LS-TaSC are discussed in sections 2.2 and 2.3.

2.1 Preliminaries

2.1.1 Isotropic elasticity

For an isotropic elastic continua, the elasticity or stiffness tensor $\boldsymbol{c}$ at a material point $\boldsymbol{x}$ is given, in component form, as

$$c_{ijkl}(\boldsymbol{x}) = \lambda(\boldsymbol{x})\delta_{ij}\delta_{kl} + \mu(\boldsymbol{x})\big(\delta_{ik}\delta_{jl} + \delta_{il}\delta_{jk}\big), \tag{1.1}$$

where λ and μ are the Lamé parameters, with the latter often referred to as the shear modulus, δ_{ij} is the Kronecker delta, i.e. $\delta_{ij} = 0$ if $i \neq j$ and $\delta_{ij} = 1$ if $i = j$, and the summation convention is used over the indices $i, j, k, l = 1, \dots, 3$. For planar elasticity, equation (1.1) holds if the first Lamé parameter is replaced with $\frac{2\lambda\mu}{\lambda+2\mu}$ [46]. Alternatively, the elasticity tensor may be expressed as

$$c_{ijkl}(\boldsymbol{x}) = \kappa(\boldsymbol{x})\delta_{ij}\delta_{kl} + \mu(\boldsymbol{x})\left(\delta_{ik}\delta_{jl} + \delta_{il}\delta_{jk} - \frac{2}{d}\delta_{ij}\delta_{kl}\right), \tag{1.2}$$

where κ is the bulk modulus and d, with $d = 2,3$, denotes the spatial dimensions. Furthermore, the relationship of the bulk and shear moduli to the Young's modulus E and the Poisson's ratio υ is written as

$$\kappa = \frac{E}{d[1-(d-1)\upsilon]}, \tag{1.3}$$

$$\mu = \frac{E}{2(1+\nu)}. \tag{1.4}$$

2.1.2 Fundamentals of mixtures

Developing computational methods to solve continuous topology design problems requires proper, i.e. constitutive, treatment of continuous mixtures of materials. The phrases composite or mixture are used interchangeably in this section. The term *mixing rule* is introduced as the description and modelling of mixtures to obtain effective material properties as function of the volume fraction of the composing material phases.

The *volume fraction* of material phase i at a material point $\boldsymbol{x} \in \Omega_D$ is denoted by $\omega_i(\boldsymbol{x})$ and represents the fraction of an infinitesimal volume element $d\Omega$ surrounding point $\boldsymbol{x}$ occupied by material phase i. Thus,

$$\omega_i = \frac{d\Omega_i}{d\Omega}, \tag{1.5}$$

where $d\Omega_i$ is the volume of the ith phase. Considering a mixture composed of n constituents, natural constraints on the volume fractions include

$$0 \leq \omega_i(\boldsymbol{x}) \leq 1 \; \forall i, \tag{1.6}$$

$$\sum_{i=1}^{n} \omega_i(\boldsymbol{x}) = 1. \tag{1.7}$$

The material volume of the ith phase within the mixture is computed as

$$\Omega_i = \int_{\Omega} \omega_i \, d\Omega. \tag{1.8}$$

The study of the set of effective material properties of a generic multiphase material, also known as the *G-closure*, and the *bounds on the effective properties* is an active area of research and plays a center role in topology and material design optimization, see e.g., [47], [48], and references therein.

The following discussion, unless otherwise stated, is confined to materials composed of two different homogeneous and isotropic elastic phases, i.e. $i = 1{,}2$. The resulting material mixtures are regarded as quasi-isotropic and quasi-homogenous. Furthermore, it is also assumed that the constituents are *well-ordered*, i.e.

$$0 < \kappa_1 \leq \kappa_2, \tag{1.9}$$

$$0 < \mu_1 \leq \mu_2, \tag{1.10}$$

where κ and μ designate the bulk and shear moduli, cf. subsection 2.1.1, and the subscript i, with $i = 1{,}2$, indicates the phases. Mixtures with non-well-ordered phases, i.e. $(\kappa_2 - \kappa_1)(\mu_2 - \mu_1) < 0$, are considered, e.g., by Walpole [49].

The G-closure of a mixture composed of two homogeneous and isotropic elastic phases is still unknown, however, optimal energy bounds allow us to derive bounds on the effective material properties of such composite, cf. section 2.3, which can be utilized in both class of continuous topology optimization [48]. The effective properties of the mixture can be characterized using, a single variable, the volume fraction of one phase. The volume fraction is often referred to as the *density variable* $\rho \in [0{,}1]$ in the topology optimization literature, i.e. equation (1.7) yields $\omega_1 = (1 - \rho)$ and $\omega_2 = \rho$, and the method is commonly referred to as the *density-based approach of topology optimization*. Depending on the value of ρ, one may distinguish void $(\rho = 0)$, intermediate $(0 < \rho < 1)$, and solid $(\rho = 1)$ phases. These phase are interchangeably identified with white, grey, and black colors, respectively. To avoid further confusion in the manuscript the dimensionless density variable or volume fraction ρ is distinguished from the material density ϱ.

2.2 Solid isotropic material with penalization

The solid isotropic material with penalization (SIMP), also called the penalized proportional fictitious material, model [50], [51] is probably the most frequently employed interpolation scheme in topology design optimization to date. In the original version of the SIMP method, a mixture of a linear isotropic elastic solid and a void phase is considered. As a simplification with respect to power law averages, see e.g., [47], however, it is assumed that the solid and void phases have equal Poisson's ratios and only the elastic modulus is interpolated, i.e.

$$E^S[\rho(\boldsymbol{x})] = \rho^p(\boldsymbol{x})E, \tag{1.11}$$

where E^S and E denote the elastic modulus of the mixture and the solid phase. The power p in equation (1.11) is a constant which is aimed at penalizing intermediate densities and therefore the constant is also called the *penalty parameter*.

A couple of things are worth highlighting at this point. First, note that the interpolation in equation (1.11) results in void and solid phases at the extreme values of ρ which means that clean solid-void designs may be obtained with the SIMP approach. Moreover, past experience with the method shows that solid-void designs can indeed be realized with the presence of the volume constraint and if the penalty parameter is sufficiently large [45]. To avoid numerical difficulties, a continuation method is often used in which the penalty parameter is gradually increased from a small value in the design cycle. Second, it is underlined that the SIMP method is a heuristic approach in the sense that it lacks exact correspondence to physically meaningful material bounds. With careful selection of the penalty parameter, however, the SIMP method can be forced to satisfy these bounds, for more details see, e.g., [3].

The SIMP method may be easily generalized for mixtures composed of two material phases such that

$$E^{GS}[\rho(\boldsymbol{x})] = E_1 + \rho^p(\boldsymbol{x})E_2, \tag{1.12}$$

where E^{GS} stands for the elastic modulus obtained by means of the generalized SIMP rule and the subscripts identify the different phases. Note that the minimum stiffness is independent of the penalty parameter in the above equation. In addition, the modified SIMP method is claimed to be easier to generalize for the use of various filtering schemes [29].

2.2.1 Extension to elasto-plasticisty

Deriving bounds on the effective properties, i.e. formulating material interpolation schemes, of elastic-plastic materials is an unsolved problem to date. It is argued, however, that exact bounds should reflect and rely on micro-mechanical considerations [45]. For instance, Mayer *et al.* [34] utilized a simple periodic porous micro-structure and computed the homogenized plastic hardening modulus based on the approximate Prandtl-Reuss equations.

A similar problem arises in stress-constrained design problems where the strength of the material needs to be interpreted at intermediate densities. As a remedy, Duysinx and Bendsøe [52] proposed an interpolation scheme for the strength in a linear elastic media based on the study of rank-2 laminates. The latter approach, also referred to as local stress interpolation, has been widely used in the recent past, see e.g., [53], [54], [55], and

[56]. The method can be generalized for piecewise linear isotropic hardening using the following interpolation scheme [38]

$$E^S[\rho(\boldsymbol{x})] = \rho^p(\boldsymbol{x})E, \tag{1.13}$$

$$\sigma_0^S[\rho(\boldsymbol{x})] = \rho^q(\boldsymbol{x})\sigma_0, \tag{1.14}$$

$$E_{H_i}^S[\rho(\boldsymbol{x})] = \rho^q(\boldsymbol{x})E_{H_i}, \tag{1.15}$$

where the newly introduced symbols σ_0, E_{H_i}, and q designate the yield strength, the strain hardening modulus associated with the ith segment of the plastic hardening curve, and a second penalty parameter. Despite the apparent lack of micro-mechanical studies, the above heuristic interpolation scheme has been successfully applied to solve large scale crashworthiness problems in LS-TaSC.

2.3 Hashin-Shtrikman bounds

The Hashin-Shtrikman bounds [57] for a two phase composite may be written as

$$\kappa_{L/U}^{HS} = \kappa_{1/2} + \frac{\omega_{2/1}}{\dfrac{1}{\kappa_{2/1} - \kappa_{1/2}} + \dfrac{\omega_{1/2}}{\kappa_{1/2} + \dfrac{4}{3}\mu_{1/2}}}, \tag{1.16}$$

$$\mu_{L/U}^{HS} = \mu_{1/2} + \frac{\omega_{2/1}}{\dfrac{1}{\mu_{2/1} - \mu_{1/2}} + \dfrac{2\omega_{1/2}\left(\kappa_{1/2} + 2\mu_{1/2}\right)}{5\mu_{1/2}\left(\kappa_{1/2} + \dfrac{4}{3}\mu_{1/2}\right)}}, \tag{1.17}$$

where the subscripts L and U indicate the lower and upper bounds, respectively.
The convex combination of the formulas $\left(\kappa_L^{HS}, \mu_L^{HS}\right)$ and $\left(\kappa_U^{HS}, \mu_U^{HS}\right)$ yields an analytical expression for the material properties of well-ordered composites with two elastic phases. More importantly, the Hashin-Shtrikman bounds represent materials that have the elastic modulus as well as the Poisson's ratio vary as a function of the volume fractions. The latter is true even if both phases have identical Poisson's ratio.
Focusing on the simplest case of topology design, the two phases represent the void (1) and solid (2) in a single material, i.e. $E_1 = 0$ and $\nu_1 = \nu_2$. For notational brevity, the subscripts are omitted and the non-zero properties are denoted by E and ν henceforth. Consequently, the Hashin-Shtrikman bounds in the different spatial dimensions take the following form

$$E_L^{HS}[\rho(\boldsymbol{x})] = \begin{cases} 0 \text{ if } \rho < 1 \\ 1 \text{ if } \rho = 1 \end{cases} \text{for } d = 2,3, \tag{1.18}$$

$$E_U^{HS}[\rho(\boldsymbol{x})] = \begin{cases} \dfrac{8E\rho(\upsilon + 17)}{21\upsilon^2(\rho - 1) + 2\upsilon(55 - 51\rho) - 123\rho + 259} & \text{if } d = 2, \\ \dfrac{2E\rho(7 - 5\upsilon)}{15\upsilon^2(\rho - 1) + 2\upsilon(\rho - 6) - 13\rho + 27} & \text{if } d = 3, \end{cases} \tag{1.19}$$

$$\upsilon_L^{HS}[\rho(\boldsymbol{x})] = \upsilon, \tag{1.20}$$

$$\upsilon_U^{HS}[\rho(\boldsymbol{x})] = \begin{cases} \dfrac{3\rho(9\upsilon^2 + 2\upsilon - 7) - 19\upsilon^2 + 130\upsilon + 21}{3\rho(7\upsilon^2 - 34\upsilon - 41) - 21\upsilon^2 + 110\upsilon + 259} & \text{if } d = 2, \\ \dfrac{\rho(5\upsilon^2 + 2\upsilon - 3) - 3(5\upsilon^2 - 4\upsilon - 1)}{\rho(15\upsilon^2 + 2\upsilon - 13) - 3(5\upsilon^2 + 4\upsilon - 9)} & \text{if } d = 3. \end{cases} \tag{1.21}$$

2.4 Material parameterization of shell structures

Topology optimization of shell structures in LS-TaSC is essentially formulated as a variable thickness sizing problem. Considering the discretized problem, the set of local design variables includes the thickness of the shell elements which parameterize the fixed design domain Ω_D. As a special case, note that variable thickness design of isotropic elastic membranes and the SIMP method with penalty parameter set to unity are equivalent and both match the Voigt upper bound [12], [58].

3
Filtering

The traditional, continuum formulation of topology optimization is prone to problems involving checkerboards, local minima, and mesh dependency in the absence of a proper regularization scheme. In the past two decades, a plethora of research works were published on regularization methods tailored to topology design, for a review the reader is advised to consult [24], [22], [29] and the references therein.

Filtering techniques can be classified as density [25], [26] and sensitivity [23] based methods. In the former case, the density of an element is typically computed as a weighted average of element densities in a mesh independent neighborhood of the element prior to solving the finite element problem and design sensitivities are modified subsequently in a consistent fashion. In the latter case, the response and sensitivity analyses are first performed in the standard and consistent way and then the design sensitivities are heuristically modified as some form of weighted average of the sensitivities in a mesh independent neighborhood.

Considering the complex and nonlinear nature of problems LS-TaSC is primarily designed for, sensitivity information is typically not available and hence we confine our discussion to density filtering. Albeit different interpolation schemes may be combined with density filtering, for simplicity piecewise constant interpolation is assumed within an element, i.e. a single density variable is associated with an element, in LS-TaSC.

Conceptually, density filters modify the density and thereby the stiffness of an element as a function of densities of adjacent elements in a predefined neighborhood, i.e.

$$\tilde{\rho}_i := \tilde{\rho}_i\left(\rho_j \in N_i\right), \tag{1.22}$$

where $\tilde{\rho}_i$ is the filtered density of the ith element, ρ_j is the original, i.e. unfiltered, density of the jth element, and N_i is the neighborhood of the ith element. The neighborhood in LS-TaSC is assumed to be spherical, and its radius is commonly referred to as the filter radius. Thus,

$$N_i = \{i \mid d_{ij} \leq r\}, \tag{1.23}$$

where d_{ij} is the distance between the centroids of element i and j, and r is the filter radius.

As a direct consequence of filtering, it is important to highlight that the original, unfiltered densities become merely intermediate variables and the filtered densities are physically meaningful. It is equally important to note that an important characteristic of filtering operators is volume conservation, I .e. the material volume should remain unchanged after the filtering. In practice, however, exact material volume preservation is rarely achieved

due to the treatment of mesh boundaries and interfaces between designed and fixed solid/void domains. This is no problem as long as the volume constraint is formulated in terms of the filtered/physical density field. For a more detailed discussion on the topic see Sigmund [29].
In what follows, we present filtering operators currently available in LS-TaSC. These filters are used to control checkerboard instabilities, as well as to drive the final solution towards a fully solid/void design. The modified version of a filter is also used to update field variables. As an example, the internal energy density field is first filtered and then used to compute the density variables in an LS-TaSC design iteration, cf. section 5.5 for more details.

3.1 Linear filter

The linear density filter [25], [26] allows us to compute the density of an element as a weighted arithmetic mean of the densities in the neighborhood of the element, i.e.

$$\tilde{\rho}_i = \sum_j w_{ij}\,\rho_j, \tag{1.24}$$

where w_{ij}, with $w_{ij} \geq 0$, $\sum_j w_{ij} = 1\ \forall i$, and $w_{ij} = 0\ \forall j \notin \mathcal{N}_i$, are weights based on volume and the distance between the neighboring elements. Depending on the choice of the weighting function, one may define various filters which may influence the efficacy and the outcome of the topology design process. This holds equally for linear and in conjunction with other filtering operators, e.g., [59]. The weighting functions available in LS-TaSC are outlined in section 3.2.

3.2 Weighting functions

The default weighting function in LS-TaSC is defined as

$$w_{ij} = \frac{v_i}{\sum_{k\in N_i} v_k}, \tag{1.25}$$

where v_i denotes the volume of the ith element. Note that averaging over the element volumes is essential in case of non-uniform meshes. Alternatively, one may use the conic function or the smoother Gaussian distribution based weights which can be written as

$$w_{ij} = \frac{v_i\left(r - d_{ij}\right)}{\sum_{k\in N_i} v_k (r - d_{ik})}, \tag{1.26}$$

$$w_{ij} = \frac{v_i e^{-\frac{1}{2}\left(\frac{d_{ij}}{\sigma}\right)^2}}{\sum_{k\in N_i} v_k e^{-\frac{1}{2}\left(\frac{d_{ik}}{\sigma}\right)^2}}, \tag{1.27}$$

where σ^2 is the variance.

4
Problem formulation

The most efficient topology optimization methods use sensitivity information e.g., optimality criterion based methods, see e.g. [1] and [3], to drive the search for an optimum. Although sensitivity calculus is computationally inexpensive for linear problems [60], its use in highly nonlinear design problems is infeasible due to the high computational cost associated with the numerical simulation. Consequently, topology crashworthiness design requires the use of alternative methods in practice. For a survey on published techniques, we refer the reader to section 1.2.
In LS-TaSC, topology design is formulated as a nested optimization including sequentially solved global and local problems. The terms global and local originate from the nature of design variables in the different steps. The set of global variables include the load case weighting factors and the mass fraction of the parts or design domains while local design variables essentially refer to the element volume fractions or densities.

4.1 The global optimization problem

The *global optimization problem* is formulated as

$$\underset{\boldsymbol{x}}{\text{minimize}}\ f[\boldsymbol{\rho}, \boldsymbol{u}^{\alpha}(\boldsymbol{\rho}), \boldsymbol{x}(\boldsymbol{\rho})] \tag{1.28}$$

$$\text{subject to } \boldsymbol{g}[\boldsymbol{\rho}, \boldsymbol{u}^{\alpha}(\boldsymbol{\rho}), \boldsymbol{x}(\boldsymbol{\rho})] \leq \mathbf{0} \tag{1.29}$$

$$\boldsymbol{x}^{L} \leq \boldsymbol{x} \leq \boldsymbol{x}^{U}, \tag{1.30}$$

where f is the objective function, $\rho \in \mathbb{R}^n$ is the set of local design or density variables, with n being the number of variables, $\boldsymbol{u}^{\alpha}$, with $\alpha = 0, \ldots, 2$, denotes the partial derivative of the displacement field with respect to time. The term $\boldsymbol{x} \in \mathbb{R}^{l+p}$ designates the set of global design variables which include the weighting factor of the different load cases and the mass fraction of the parts or design regions, i.e. $\boldsymbol{x} = (w_1, \ldots, w_l, \chi_1, \ldots, \chi_p)$ where w_i is the weighting factor of the ith load case, χ_j is the mass fraction of the jth part with l and p denoting the number of load cases and parts, respectively. For notational brevity, we also introduce the symbols $\boldsymbol{w} \in \mathbb{R}^l$ and $\boldsymbol{\chi} \in \mathbb{R}^p$ to denote the set of load case weighting factors and part mass fractions. The symbol $\boldsymbol{g} \in \mathbb{R}^m$ in equation (1.29) stands for the structural and other constraints with m representing the number of constraints. Finally, $\boldsymbol{x}^L$ and $\boldsymbol{x}^U$ in

equation (1.30) designate the lower and upper bounds on the global variables. For clarity, the *mass fraction* is defined as the ratio of the current and target masses, i.e.

$$\chi_i(\boldsymbol{\rho}) = \frac{m_i(\boldsymbol{\rho})}{\overline{m}_i}, \tag{1.31}$$

where the newly introduced symbols m_i, and $\overline{m}_i$ denote the current and the target masses of the ith part, respectively.

4.2 The local design problem

Considering the *local optimization problem*, we rely on the formulation originally proposed by Patel [38] and set the objective of the design problem to obtain uniform internal energy density in the structure. Thus, the local optimization problem for a single design region can be written as

$$\underset{\boldsymbol{\rho}}{\text{minimize}} \sum_{i=1}^{l}\sum_{j=1}^{n} w_i\left[U_{ij}(\rho) - \overline{U}_i\right] \tag{1.32}$$

$$\text{subject to } \chi(\boldsymbol{\rho}) - 1 \leq 0 \tag{1.33}$$

$$\boldsymbol{\rho}^L \leq \boldsymbol{\rho} \leq \mathbf{1}, \tag{1.34}$$

where U_{ij} is the internal energy density of the jth element in the ith load case, $\overline{U}_i$ is the target internal energy density in the ith load case. Bounds on the local design variables are given in equation (1.34) where the lower bound is customarily set to a small positive value, i.e. $0 < \rho_j^L = \varepsilon \ll 1$, in order to inhibit a singular finite element formulation.

A few things are worth highlighting at this point. First, updating the global design variables by solving a mathematical programming problem is a new feature in LS-TaSC 3.1. Past releases of LS-TaSC employed a control theory based update procedure, cf. section 5.3, which is still included and maintained in the current version. Second, the objective and/or constraints in both design problems are, explicitly or implicitly, functions of the local as well as the global design variables. Third, the target internal energy density in the local optimization problem, see equation (1.32), is computed internally based on the load case weighting factors and the mass fraction in the current iteration. Fourth, the above optimization problem only includes a single design region, e.g., component or preselected section of an assembly, for which the target mass and internal energy densities are set. This simplification, however, is merely done for easier readability and there is no limitation on the number of user defined design regions.

5
Design algorithm

The optimization problem, as formulated in section 4, is solved by the LS-TaSC topology design algorithm. The present implementation of LS-TaSC relies on a different solution scheme compared to what was originally proposed by Tovar [61] and Patel [38]. Next to several new features and enhancements in the current version, the key differences include

1. the elimination of cellular automaton based update rules;
2. the definition of several update strategies for the load case weighting factors and the target mass;
3. the extension to a more general design formulation through the support for general structural and non-structural constraints;
4. substructuring capabilities, and the ability to exactly satisfy multiple constraints at once;
5. an algorithm that converts regions of intermediate densities into a clean solid/void designs.

The flowchart of the LS-TaSC design algorithm is illustrated in Figure 1-1. In what follows, the main steps of the algorithm are discussed in more detail.

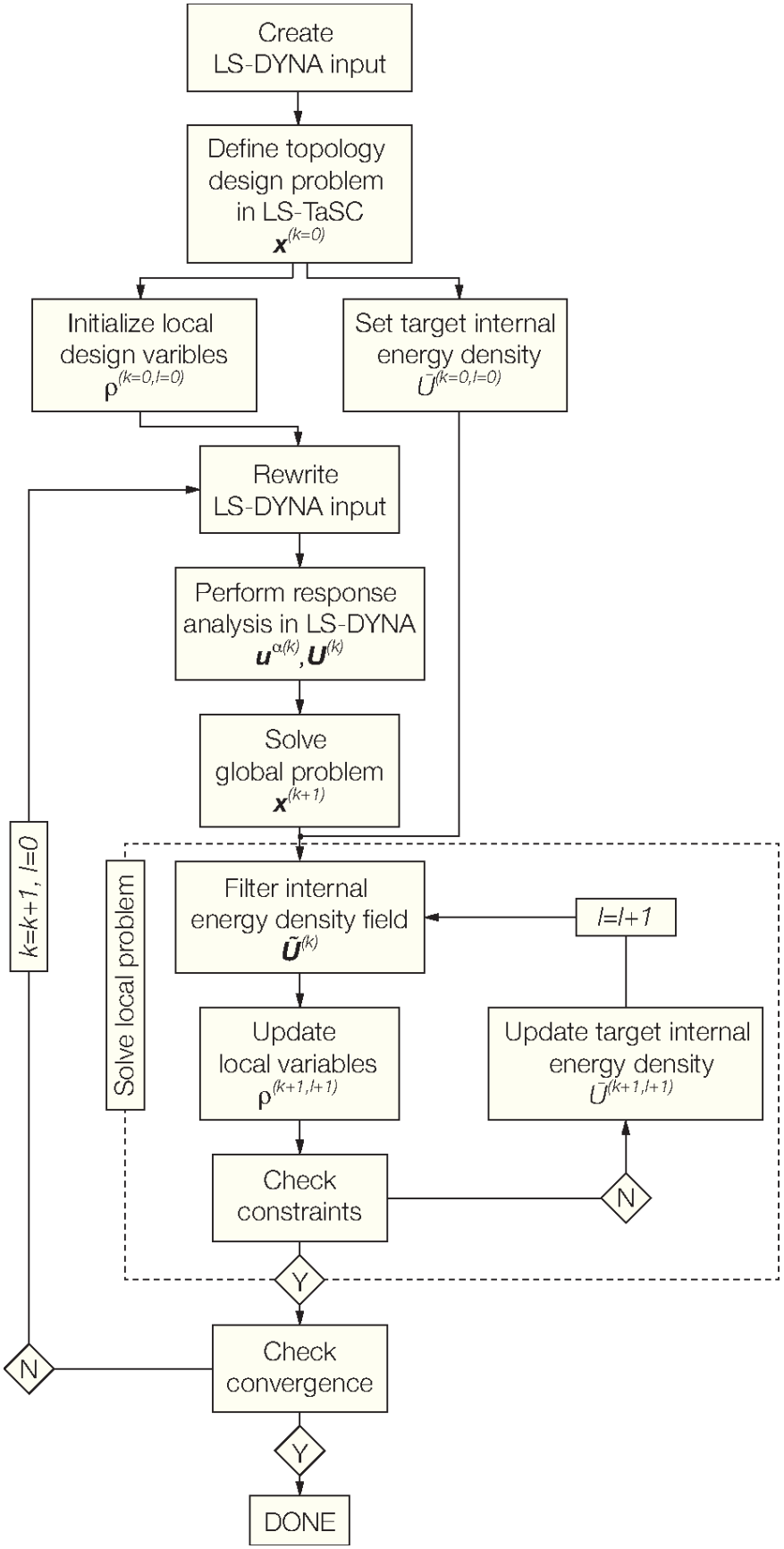

Figure 1-1. The LS-TaSC design algorithm.

5.1 Design initialization

Global design variables need to be initialized by the user. Conversely, local design variables are initialized automatically to satisfy the constraint on the structural mass given in equation (1.33). Thus, assuming uniform density for the jth part or design domain

$$\rho_i = \frac{\bar{m}_j}{\varrho_j v_i}, \tag{1.35}$$

where ρ_i is the density variable of the ith element, $\bar{m}_j$ is the target mass of the jth part, ϱ_j is the density of material in the jth part, and v_i is the volume of the ith element. Note that equation (1.35) yields uniform density distribution on uniform meshes.

User defined geometric or manufacturing constraints on the geometry are treated automatically within LS-TaSC. For instance, extrusion, symmetry, or casting definitions result in additional equality or inequality constraints between the design variables.

5.2 Response analysis

The physical problem at hand is solved using a numerical method in LS-DYNA [62]. In what follows, we restrict the discussion to the finite element method as it is the most frequently used numerical scheme in the structural synthesis. However, one needs to bear in mind that an alternative numerical technique may be better suited to simulate the physical problem at hand.

As discussed previously, the local design variables or densities are used to rescale the stiffness properties of the elements. In LS-TaSC this is simply achieved by modifying the constitutive or material models[1]. This is done in uniform discrete steps that may be defined by the user. Material cards corresponding to discrete density values are written to a separate LS-DYNA input file prior to the initial finite element run [63].

Considering uniform meshes, initially the same material card is assigned to each element as discussed in section 5.1. The internal energy density field, obtained as a result of the finite element analysis, is used to update the local design variables. This is described in more detail in section 5.5. Upon updating the local design variables a new material card is assigned to each element in LS-TaSC and the LS-DYNA input deck is rewritten. This modified input is analyzed at the beginning of a new iteration. Here one can take advantage of multiple processors using the MPP version of LS-DYNA.

In addition, elements may also be added or deleted in each iteration. An element is added within the predefined design domain, if its filtered density, cf. section 5.5, surpasses the lower bound of the density given in equation (1.34). An element with density below the threshold may be deleted or kept with stiffness properties scaled with the threshold value of the density.

[1] Note that only a subset of materials from the otherwise extensive material library of LS-DYNA [28] is supported in LS-TaSC.

5.3 Global variable update using control theory

The update of global variables using control theory was implemented in previous versions of LS-TaSC. These heuristic update rules evolved empirically based on past experience on large-scale industrial problems and are recapitulated in this section. It is remarked, however, that the use of mathematical programming introduced in LS-TaSC 3.1 provides a far more flexible and general approach to adjust the global variables, cf. section 5.4 for more details.

In the presence of general constraints, the load factor weight factors and the target masses are adjusted in the following ways. The weighting factor of the ith load case is updated as

$$w_i^{(k+1)} = w_i^{(k)} + \Delta w_i, \tag{1.36}$$

where the superscripts in parentheses indicate the iteration number and Δw_i is the change in the ith weighting factor. The desired behavior can be obtained as

$$\alpha_i g_i^{(k)} + \delta_i = \alpha_j g_j^{(k)} + \delta_j \quad \text{with } i, j = 1, \dots, m \text{ and } i \neq j, \tag{1.37}$$

where α_i and δ_i are the scaling and shifting parameters associated with the ith constraint $g_i^{(k)}$. The change in the load case weights is computed as

$$\Delta w_i = \frac{\gamma\left[\,\overline{g}^{(k)} - \alpha_i g_i^{(k)} - \delta_i\right]^{(k)}}{\overline{g}^{(k)}} \quad \forall i, \tag{1.38}$$

where $\gamma \in \mathbb{R}^+$ is a scaling parameter and $\overline{g}^{(k)}$ is the average of the scaled and shifted constraint values, i.e.

$$\overline{g}^{(k)} = \frac{1}{m}\sum_{i=1}^{m}\left[\alpha_i g_i^{(k)} + \delta_i\right]. \tag{1.39}$$

Furthermore, the change in the load case weights is bound to ensure convergence in a reasonable number of iterations such that

$$\Delta w_i = \begin{cases} \max\left[-0.05 w_i^{(k)}, \Delta w_i\right] & \text{if } \Delta w_i \leq 0 \\ \min\left[\Delta w_i, 0.05 w_i^{(k)}\right] & \text{if } \Delta w_i > 0. \end{cases} \tag{1.40}$$

The target mass of the part is adjusted to satisfy the structural and other constraints. To this end, the target mass is increased or decreased in proportion to the constraint violation for displacement or force based constraints, respectively. Thus,

$$\overline{m}^{(k+1)} = \overline{m}^{(k)} + \Delta\overline{m}, \tag{1.41}$$

where $\Delta\overline{m}$ is the change in the target mass defined as

$$\Delta\overline{m} = \frac{1}{m}\sum_{i=1}^{v}\beta_i g_i^{(k)}, \tag{1.42}$$

where m is the number of constraints, v is the number of violated constraints, i.e. $g_i^{(k)} > 0$, and β_i is a coefficient used to scale the ith constraint. Similarly to the update of the load case weights in equation (1.40), the change in target mass is also bounded to allow gradual changes in the structure.

5.4 Global variable update via mathematical programming

Starting with LS-TaSC 3.1, global variables may as well be updated by solving the mathematical programming problem outlined in section 4.1. This allows the designer to define and handle problems of greater complexity in a natural and mathematically sound fashion. More importantly, the method lends itself to include multiple parts or domains within the design formulation.

The mathematical programming problem in equations (1.28)-(1.30), can be solved using sequential approximations, e.g., sequential linear programming, which require the sensitivity of the objective and constraint functions with respect to the global design variables. These derivatives may be computed by either finite differences [60] or linear metamodels [64] in LS-TaSC. Sensitivities may be computed in predefined intervals comprising multiple design iterations. Furthermore, to account for the nature of nonlinear dynamic processes, the sensitivity may be computed as an average over the previous iterations, i.e.

$$\frac{\partial f^{(k)}}{\partial x} = \frac{1}{n+1}\sum_{i=0}^{n}\frac{\partial f^{(k-i)}}{\partial x}, \tag{1.43}$$

where f and x denote an arbitrary function and global design variable, n designates the number of previous iterations (or intervals) taken into account to compute the sensitivity in the kth iteration. One motivation of sensitivity averaging or damping is to prevent problems with gradients that change their sign between successive iterations.

In addition, move limits are imposed on the global design variables. The move limits are centered around the global variables obtained previous iteration. Hence, the update is given as

$$x^{(k+1)} = \begin{cases} \min\left[\mu x^{(k)}\left(1-e^{\frac{k}{10}}\right), x^{(k)}+\Delta x\right] & \text{if } \Delta x \le 0 \\ \max\left[\mu x^{(k)}\left(1+e^{\frac{k}{10}}\right), x^{(k)}+\Delta x\right] & \text{if } \Delta x > 0, \end{cases} \tag{1.44}$$

where μ is a scaling factor, which is set differently for load case weights and mass fractions, and Δx is the solution of the global optimization problem.

5.5 Local variable update

The local optimization problem is solved iteratively using a zeroth-order method that contains three main steps. In the first step, the internal energy density field is filtered. Next, the local variables are updated based on the filtered internal energy densities. Finally, the constraint of the resulting mass fraction is evaluated. If the constraint in equation (1.33) is satisfied the algorithm terminates, else the target internal energy density is readjusted and a new iteration is started. The local update scheme is depicted in Figure 1-1.

Filtering the internal energy density field is done through the consecutive use of a spatial and a temporal filter. Assuming a uniform mesh and following the spirit of equations (1.24) and (1.25), the spatial filter is written as

$$\widetilde{U}_i = \frac{1}{e}\sum_{j\in N_i} U_j, \tag{1.45}$$

where $\widetilde{U}_i$ is the filtered internal energy density and e denotes the total number of elements within the filter radius of the ith element. The temporal filter is motivated by the observation that accounting for evolution of the internal energy field reduces the element deletion rate and thereby improves the stability of the computation. Analogously to equation (1.43), the internal energy density field is averaged as

$$\widetilde{U}_i^{(k)} = \frac{1}{n+1}\sum_{j=0}^{n} \widetilde{U}_i^{(k-j)}, \tag{1.46}$$

where n denotes the number of previous iterations considered.
Once the internal energy density field is filtered, the local design variables are adjusted to reflect the changes. While numerous rules are proposed to update the local design variables in the literature, e.g., see [3], a control theory inspired scheme is implemented here after Patel [38]. Hence, a density variable is modified as

$$\rho_i^{(k+1,l)} = \rho_i^{(k,l)} + \Delta\rho^{(k,l)}, \tag{1.47}$$

where the superscript l denotes the number of iterations in the local problem in which the target internal energy density value is adjusted, and $\Delta\rho$ is the change in density. The latter is computed as

$$\Delta\rho^{(k,l)} = \mu\left(\psi^{(k,l)} - 1\right), \tag{1.48}$$

where μ is a scaling factor and ψ is the (filtered) internal energy density fraction defined, analogously to equation (1.31), as the ratio of current and target internal energy densities. If the updated density variable $\rho_i^{(k+1,l)}$ exceeds the bounds given in equation (1.34), the density is reset to the value of the violated bound.

5.5.1 Internal energy density – two interpretations

Considering solid elements, the internal energy density is defined differently in LS-DYNA and LS-TaSC. LS-DYNA stores the internal energy density values relative to the volume of the element in the *d3plot* files. Conversely, the internal energy density is defined and used per material volume in LS-TaSC. Using the definition of material volume, see in equation (1.8), the internal energy density per element volume needs to be scaled with ρ^{-1} to obtain the internal energy density per material volume. Generally, this difference only applies to energy density computations. Energies reported in the *glstat* files are always unscaled. The above difference does not apply for topology design of shell structures. There, the set of design variables comprises the thickness of the shell elements, see section 2.4.

5.6 Stopping criteria

An optimization cycle in LS-TaSC is terminated either if the maximum number of iterations is exceeded or if the change in the topology is below a predefined tolerance. To account for eventual numerical oscillations, the change in topology is defined as the average of the changes in the current and previous iterations. Hence, the criterion on the change in topology can be written as

$$\frac{1}{2}\sum_{j=0}^{1}\sum_{i}\Delta\rho_i^{(k-j,l)} \leq \varepsilon, \tag{1.49}$$

where $\varepsilon \in \mathbb{R}^+$ is the tolerance on the change in topology. Satisfying any of the convergence criteria terminates the optimization cycle.

6 References

[1] G. I. N. Rozvany, Structural design via optimality criteria, Dordrecht: Kluwer Academic Publishers, 1989.

[2] G. I. N. Rozvany and N. Olhoff, Topology optimization of structures and composite continua, Dordrecht: Kluwer Academic Publishers, 2000.

[3] M. P. Bendsøe and O. Sigmund, Topology optimization: Theory, methods and applications, Heidelberg: Springer-Verlag Inc., 2003.

[4] H. A. Eschenauer and N. Olhoff, "Topology optimization of continuum structures: A review," *Applied Mechanics Reviews,* vol. 54, no. 4, pp. 331-390, 2001.

[5] N. P. van Dijk, K. Maute and F. van Keulen, "Level-set methods for structural topology optimization: a review," *Structural and Multidisciplinary Optimization,* vol. 48, pp. 437-472, 2013.

[6] K. A. Lurie, Applied optimal control theory of distributed systems, New York: Plenum Press, 1993.

[7] M. Beckers, "Topology optimization using a dual method with discrete variables," *Structural Optimization,* vol. 17, pp. 14-24, 1999.

[8] R. V. Kohn and G. Strang, "Optimal design and relaxation of variational problems, I," *Communications on Pure and Applied Mathematics,* vol. 39, no. 1, pp. 113-137, 1986.

[9] R. V. Kohn and G. Strang, "Optimal design and relaxation of variational problems, II," *Communications on Pure and Applied Mathematics,* vol. 39, no. 2, pp. 139-182, 1986.

[10] R. V. Kohn and G. Strang, "Optimal design and relaxation of variational problems, III," *Communications on Pure and Applied Mathematics,* vol. 39, no. 3, pp. 353-377, 1986.

[11] K.-T. Cheng and N. Olhoff, "An investigation concerning optimal design of solid elastic plates," *International Journal of Solids and Structures,* vol. 17, no. 3, pp. 305-323, 1981.

[12] C. C. Swan and I. Kosaka, "Voigt-Reuss topology optimization for structures with linear elastic material behaviours," *International Journal for Numerical Methods in*

Engineering, vol. 40, pp. 3033-3057, 1997.

[13] M. P. Bendsøe and N. Kikuchi, "Generating optimal topologies in structural design using a homogenization method," *Computer Methods in Applied Mechanics and Engineering,* vol. 71, pp. 197-224, 1988.

[14] C. S. Jog, R. B. Haber and M. P. Bendsøe, "Topology design with optimized self-adaptive materials," *International Journal of Numerical Methods in Engineering,* vol. 37, no. 8, pp. 1323-1350, 1994.

[15] H. Gea and Y. Fu, "3-D shell topology optimization using a design domain method," *SAE Technical Paper 951105,* pp. 245-251, 1995.

[16] O. Sigmund, "A new class of extremal composites," *Journal of the Mechanics and Physics of Solids,* vol. 48, pp. 397-428, 2000.

[17] J. Petersson and O. Sigmund, "Slope constrained topology optimization," *International Journal for Numerical Methods in Engineering,* vol. 41, no. 8, pp. 1417-1434, 1998.

[18] M. Zhou, Y. K. Shyy and H. L. Thomas, "Checkerboard and minimum member size control in topology optimization," *Structural and Multidisciplinary Optimization,* vol. 21, pp. 152-158, 2001.

[19] L. Ambrosio and G. Buttazzo, "An optimal design problem with perimeter penalization," *Calculus of Variations and Partial Differential Equations,* vol. 1, no. 1, pp. 55-69, 1993.

[20] R. B. Haber, C. S. Jog and M. P. Bendøe, "A new approach to variable-topology shape design using a constraint on perimeter," *Structural Optimization,* vol. 11, no. 1-2, pp. 1-12, 1996.

[21] T. Borrvall and J. Petersson, "Topology optimization using regularized intermediate density control," *Computational Methods in Applied Mechanics and Engineering,* vol. 190, pp. 4911-4928, 2001.

[22] T. Borrvall, "Topology optimization of elastic continua using restriction," *Archives of Computational Methods in Engineering,* vol. 8, no. 4, pp. 351-385, 2001.

[23] O. Sigmund, "On the design of compliant mechanisms using topology optimization," *Mechanics of Structures and Machines,* vol. 25, no. 4, pp. 493-524, 1997.

[24] O. Sigmund and J. Petersson, "Numerical instabilities in topology optimization: A survey on procedures dealing with checkerboards, mesh-dependencies and local minima," *Structural Optimization,* vol. 16, no. 1, pp. 68-75, 1998.

[25] T. E. Bruns and D. A. Tortorelli, "Topology optimization of non-linear elastic structures and compliant mechanisms," *Computer Methods in Applied Mechanics and Engineering,* vol. 190, no. 26-27, pp. 3443-3459, 2001.

[26] B. Bourdin, "Filters in topology optimization," *International Journal for Numerical Methods in Engineering,* vol. 50, no. 9, pp. 2143-2158, 2001.

[27] J. A. Sethian and A. Wiegmann, "Structural boundary design via level set and immersed interface methods," *Journal of Computational Physics,* vol. 163, no. 2, pp. 489-528, 2000.

[28] B. Bourdin and A. Chambolle, "Design-dependent loads in topology optimization," *ESAIM: Control, Optimisation and Calculus of Variations,* vol. 9, pp. 19-48, 2003.

[29] O. Sigmund, "Morphology-based black and white filters for topology optimization,"

Structural and Multidisciplinary Optimization, vol. 33, no. 5, pp. 401-424, 2007.

[30] O. Sigmund and S. Torquato, "Design of smart composite materials using topology optimization," *Smart Materials and Structures,* vol. 8, pp. 365-379, 1999.

[31] N. M. Patel, B.-S. Kang, J. E. Renaud and A. Tovar, "Crashworthiness design using topology optimization," *Journal of Mechanical Design,* vol. 131, no. 6, 2009.

[32] Livermore Software Technologies Corporation, LS-OPT User's Manual, Livermore, 2015.

[33] C. A. Soto, "Structural topology optimization for crashworthiness," *International Journal of Crashworthiness,* vol. 9, no. 3, pp. 277-283, 2004.

[34] R. R. Mayer, N. Kikuchi and R. A. Scott, "Application of topological optimization techniques to structural crashworthiness," *International Journal for Numerical Methods in Engineering,* vol. 39, no. 8, pp. 1383-1403, 1996.

[35] C. B. W. Pedersen, "Topology optimization design of crushed 2D-frames for desired energy absorption history," *Structural and Multidisciplinary Optimization,* vol. 25, no. 5-6, pp. 368-382, 2003.

[36] C. B. W. Pedersen, "Crashworthiness design of transient frame structures using topology optimization," *Computer Methods in Applied Mechanics and Engineering,* vol. 193, no. 6-8, pp. 653-678, 2004.

[37] T. Ebisugi, H. Fujita and G. Watanabe, "Study of optimal structure design method for dynamic nonlinear problem," *JSAE Review,* vol. 19, no. 3, pp. 251-255, 1998.

[38] N. M. Patel, Crashworthiness design using topology optimization, PhD thesis: University of Notre Dame, 2007.

[39] J. Forsberg and L. Nilsson, "Topology optimization in crashworthiness design," *Structural and Multidisciplinary Optimization,* vol. 33, no. 1, pp. 1-12, 2007.

[40] M. Öman and L. Nilsson, "Structural optimization of product families subjected to multiple crash load cases," *Structural and Multidisciplinary Optimization,* vol. 41, no. 5, pp. 797-815, 2010.

[41] M. Öman and L. Nilsson, "Structural optimization based on internal energy distribution," *Engineering Optimization,* vol. 45, no. 4, pp. 397-414, 2013.

[42] P. S. Motamarri, A. Ramani and A. Kaushik, "Structural topology synthesis with dynamics and nonlinearities using equivalent linear systems," *Structural and Multidisciplinary Optimization,* vol. 45, no. 4, pp. 545-558, 2012.

[43] A. Ramani and A. Kaushik, "Topology optimization for nonlinear dynamic problems: Considerations for automotive crashworthiness," *Engineering Optimization,* vol. 46, no. 4, pp. 487-502, 2014.

[44] K. Witowski, H. Müllerschön, A. Erhart, P. Schumacher and K. Anakiev, "Topology and topometry optimization of crash applications with the equivalent static load method," in *13 th International LS-DYNA Users Conference*, Dearborn, MI, 2014.

[45] M. P. Bendsøe and O. Sigmund, "Material interpolation schemes in topology optimization," *Archive of Applied Mechanics,* vol. 69, pp. 635-654, 1999.

[46] I. S. Sokolnikoff, Mathematical theory of elasticity, New York: McGraw-Hill Publishing Company Ltd., 1956.

[47] A. V. Cherkaev, Variational methods for structural optimization, New-York: Springer-Verlag Inc., 2000.

[48] G. Allaire, Shape optimization by the homogenization method, New York: Springer-Verlag Inc., 2002.

[49] L. J. Walpole, "On bounds for overall elastic moduli of inhomogeneous systems," *Journal of the Mechanics and Physics of Solids,* vol. 14, pp. 151-162, 1966.

[50] M. P. Bendsøe, "Optimal shape design as a material distribution problem," *Structural Optimization,* vol. 1, no. 4, pp. 193-202, 1989.

[51] M. Zhou and G. I. N. Rozvany, "The COC algorithm, Part II: Topological, geometrical and generalized shape optimization," *Computer Methods in Applied Mechanics and Engineering,* vol. 89, no. 1-3, pp. 309-336, 1991.

[52] P. Duysinx and M. P. Bendsøe, "Topology optimization of continuum structures with local stress constraints," *International Journal for Numerical Methods in Engineering,* vol. 43, no. 9, pp. 1453-1478, 1998.

[53] J. T. Pereira, F. E. A and C. S. Barcellos, "Topology optimization of continuum structures with material failure constraints," *Structural and Multidisciplinary Optimization,* vol. 26, no. 1, pp. 50-66, 2004.

[54] M. Bruggi, "On an alternative approach to stress constraint relaxation in topology optimization," *Structural and Multidisciplinary Optimization,* vol. 36, no. 2, pp. 125-141, 2008.

[55] J. París, F. Navarrina, I. Colominas and M. Casteleiro, "Topology optimization of continuum structures with local and global stress constraints," *Structural and Multidisciplinary Optimization,* vol. 39, no. 4, pp. 419-437, 2009.

[56] Y. Luo and Z. Kang, "Topology optimization of continuum structures with Drucker-Pragner yield stress constraints," *Computers and Structures,* Vols. 90-91, pp. 65-75, 2012.

[57] Z. Hashin and S. S, "A variational approach to the theory of the elastic behaviour of multiphase materials," *Journal of the Mechanics and Physics of Solids,* vol. 11, pp. 127-140, 1963.

[58] C. C. Swan and I. Kosaka, "Voigt-Reuss topology optimization for structures with nonlinear material behaviors," *International Journal for Numerical Methods in Engineering,* vol. 40, pp. 3785-3814, 1997.

[59] K. Svanberg and H. Svärd, "Density filters for topology optimization based on the geometric and harmonic means," in *10th World Congress on Structural and Multidisciplinary Optimization*, Orlando, FL, 2013.

[60] R. T. Haftka and Z. Gürdal, Elements of structural optimization, Dordrecht: Kluwer Academic Publishers, 1992.

[61] A. Tovar, Bone remodelling as a hybrid cellular automaton optimization process, PhD thesis: University of Notre Dame, 2004.

[62] Livermore Software Technology Corporation, LS-DYNA Theory Manual, Livermore, 2015.

[63] Livermore Software Technology Corporation, LS-DYNA Keyword User's Manual, Volume I, Livermore, 2015.

[64] T. W. Simpson, J. D. Poplinski, P. N. Koch and J. K. Allen, "Metamodels for computer-based engineering design: survey and recommendations," *Engineering with Computers,* vol. 17, no. 2, pp. 129-150, 2001.

[65] Livermore Software Technology Corporation, LS-DYNA Keyword User's Manual, Volume II - Material Models, Livermore, 2015.